2010

Comparative Experimental Study on Wear Resistance of Different Types of Star Wheels in the Single Screw Compressor

Jian Li
School of Energy and Power Engineering

Xiaoling Yu
School of Energy and Power Engineering

Bo Hu
School of Energy and Power Engineering

Quanke Feng
School of Energy and Power Engineering

Comparative Experimental Study on Wear Resistance of Different Types of Star Wheels in the Single Screw Compressor

Jian Li[1]*, Xiaoling Yu[1], Bo Hu[1], Quanke Feng[1]

[1]School of Energy and Power Engineering, Xi'an Jiaotong University
Xi'an, 710049, China
86-29-82675258, Fax: 86-29-82663783, lijianxjtu@gmail.com

* Corresponding Author

ABSTRACT

Single screw compressors (SSCs) have been used in many fields. Compared with other kinds of compressors, the SSC should have many advantages due to its symmetrical structure and well balanced radial gas pressure on the screw rotor. However, its durability is not as good as expected. After operating for several thousand hours, its flow rate often decreases sharply. The essential reason is that the tooth flank of its star wheels is easily worn. In order to improve the wear resistance and operation life of the SSC, some new types of meshing pairs have been proposed. In this paper, we designed and made an eccentric wheel friction test device.

In the test an eccentric wheel was used to wear samples of different meshing pairs. The wearing mechanism can ensure the angle between the sample and the surface of the eccentric wheel is similar to that between the star wheel blade and the screw groove surface. The test compared the erosion amounts of different star wheel profiles: single straight line, multi straight lines, cylinder, and single straight line second envelop meshing pairs. Results show that dispersing the abrasion area and making the load transition continuous and steady can improve wear resistance.

1. INTRODUCTION

Single screw compressors (SSCs), developed in the 1960's (Zimmern *et al.*, 1972), have been used in many fields, such as power, refrigeration, air conditioning, petroleum and chemistry plants (Wu and Tao, 2006). The typical structure of a SSC is shown in Fig. 1. It mainly consists of a screw rotor and two symmetrical star-wheels. Compared with other kinds of compressors, SSC should have many advantages due to its symmetrical structure and well balanced radial gas pressure on the screw rotor. However, its durability is not as good as expected. After operating for hundreds hours, its flow rate often decreases sharply (Zimmern *et al.*, 1972). The essential reason is that the tooth flank of its star wheels is easily worn (Zimmern, 1990). Applying high wear-resistance material such as polyether-ether-ketone (PEEK) and improving machining precision can help to prolong the life of SSCs, but it does not resolve this issue efficiently. Besides the material and precision, meshing pair profile is the basic factor affecting the wear resistance (Zimmern, 2000). Therefore, some scholars try to find an excellent meshing pair profile to reduce the friction between the two components of the meshing pair.

The original meshing pair profile is a straight-line envelope type, which was invented by Zimmern in 1960s. The contact line between the meshing pair on star-wheel tooth flank is a fixed straight line. Zimmern (1976) developed a column (frustum) envelope meshing pair. The contact line between the meshing pair moves on the star-wheel tooth flank. A straight line double envelope meshing pair and a column (frustum) double envelope meshing pair were introduced in the 1980s (Jin, 1982; Jin and Tang, 1985). The double envelope means using the straight line or column (frustum) enveloped surface of the screw rotor groove flank as a generating tool to envelop the star-wheel tooth flank.

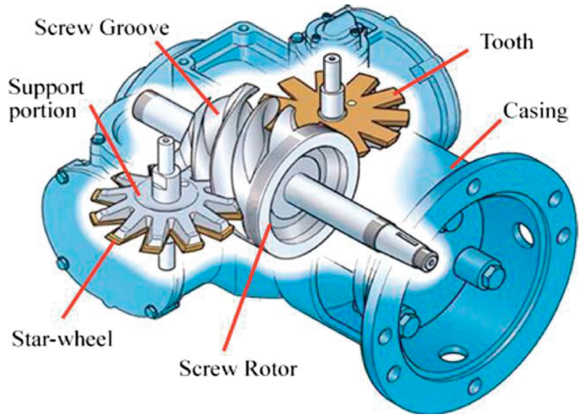

Fig. 1 Basic components of a typical single screw compressor

Feng *et al.* (2005) deduced a multi-straight line envelope meshing pair. It used more than two straight lines with different positions and directions on the star-wheel tooth together to envelop a groove flank on the screw rotor. The contact line of the meshing pair switches in these straight lines on star-wheel tooth flank. Wu and Feng (2009) deduced a multi-column envelope meshing pair, which was based on the column envelope (Zimmern, 1990) and multi- straight line envelope (Feng *et al.* 2005) meshing pairs [6]. The star-wheel tooth flank consisted of more than two parts of cylindrical segments, which mesh with the screw rotor groove flank alternately.

This paper presents an eccentric wheel friction test device, which we designed to compare the wear behavior of the star-wheel in different meshing pair profiles.

2. THE ECCENTRIC WHEEL FRICTION TEST DEVICE

In the test an eccentric wheel was used to wear samples of different meshing pairs. The wearing mechanism can ensure the angle between the sample and the surface of the eccentric wheel is similar to that between the star wheel blade and the screw groove surface.

2.1 The Mathematical Model of the Test Device

When one flank of a star-wheel tooth contacts the screw groove flank, there is a contact line between the meshing pair on the star-wheel tooth flank. Fig. 2 shows that A is any point in the contact line and α is the envelope angle of the point. Because the tooth flank moves tangentially with the groove flank, the relative velocity of the tooth flank to the groove flank must be orthogonal to the normal vector of the tooth flank at the contact point (Kang *et al.* 1996). Therefore, the envelope angle of contact point A is expressed as

$$\alpha = \arctan(\frac{U_{R_A}}{U_{r_A}}) = \arctan(\frac{R_A \cdot \omega_R}{r_A \cdot \omega_r}) = \arctan(\frac{H - r_A \cdot \sin\theta}{r_A} \cdot \frac{Z_r}{Z_R}) \tag{1}$$

Where, U is the velocity; ω is the angular velocity; R_A, r_A denote the radii; H is the central moment between the meshing pair; θ is the star-wheel rotation angle; Z is the teeth number; subscripts 'R' and 'r' denote the screw rotor and the star-wheel; subscript 'A' denotes the contact point A.

In this work, a numerical example is presented in Table 1. Thus, as shown in Fig. 3, the envelope angle changes with the star-wheel rotation angle. When the contact point moves from the root to the top of the star-wheel teeth, the variation ranges of the envelope angle become smaller. The largest envelope angle variation range is on the top of the star-wheel tooth flank. So, this position will be worn more easily.

Table 1: Major design parameters of an example SSC

H/mm	R/mm	r/mm	Z_R	Z_r
185	115	115	6	11

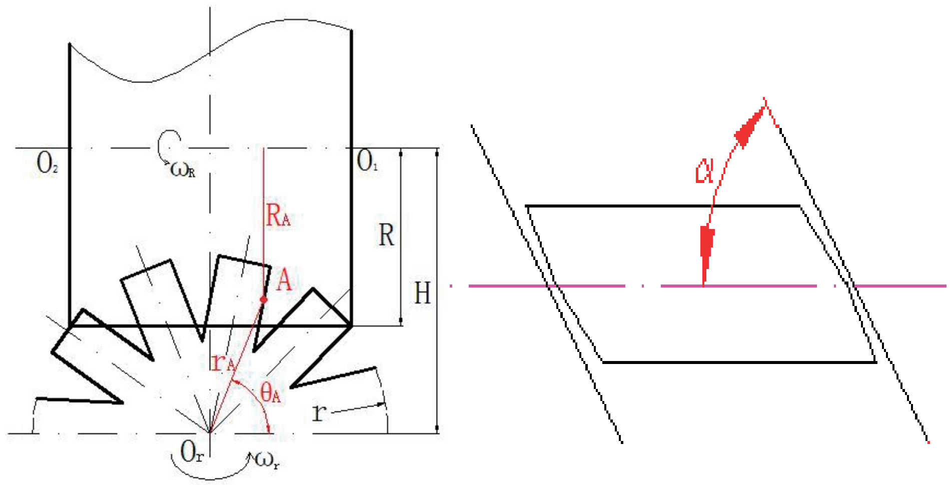

(a) (b)

Fig. 2 A point in the contact line and the envelope angle

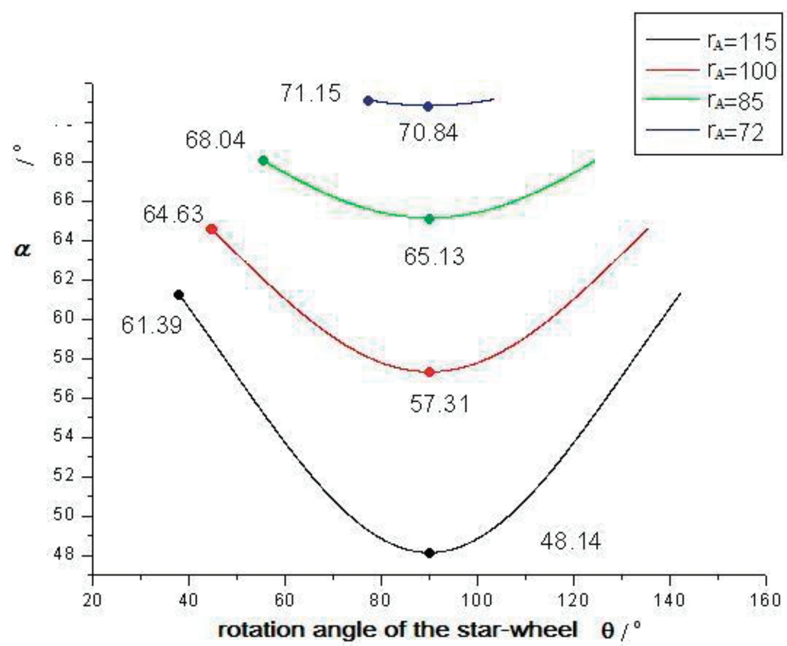

Fig. 3 Changes of envelope angle at different points in the contact line

2.2 The design of the test setup

The principle of the test device is shown in Fig. 4. An eccentric wheel is used to wear samples of different meshing pairs. The meshing profiles of the samples are similar to that of the different types of star-wheel tooth flanks. O is the rotation center of the eccentric wheel; O' is the circle center; R is the radius; d is the eccentricity; L is the vertical distance between O and the direction line of the sample, which is through the contact point; θ is the rotation angle. So the envelope angle of the wearing mechanism α is

$$\alpha = \arctan\left(\frac{\sqrt{R^2-(L-d\cdot\cos\theta)^2}+d\sin\theta}{L}\cdot\right) \tag{2}$$

Thus, choosing appropriate R, d, L can make the variation range of α the same as the envelope angle change range in the SSCs. In this test, the test device was reformed by a V-type piston compressor, as shown in Fig. 5.

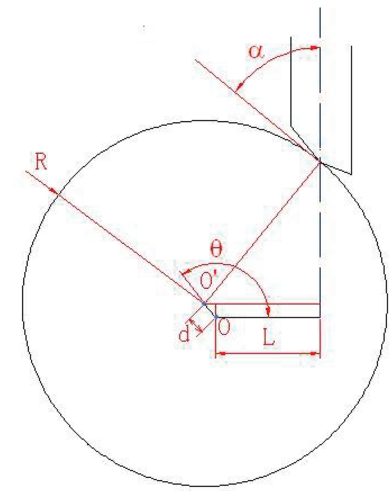

Fig.4 The schematic diagram of the test

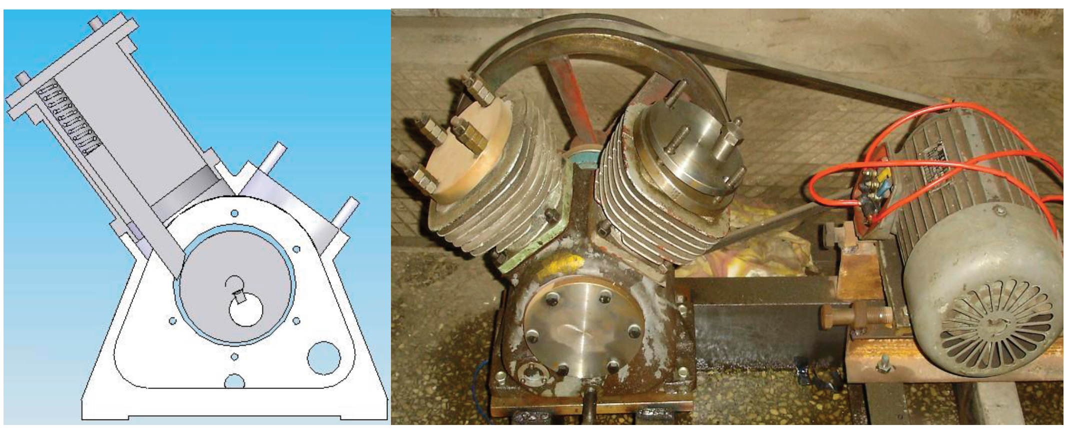

Fig.5 The structure of the test

The top of the star-wheel tooth flank will be worn more easily. At this position of the example SSC, the envelope angle variation range is 48.14°~61.39°, as shown in Fig. 3. Then we chose *R*=54mm, *d*=9mm, *L*=30mm. So, the variation range of α in this test is 48.19°~61.56°, as shown in Fig. 6. The two envelope angle variation ranges are very similar. Therefore, the test setup can be used to simulate the wear characteristics of the top of the star-wheel tooth flank.

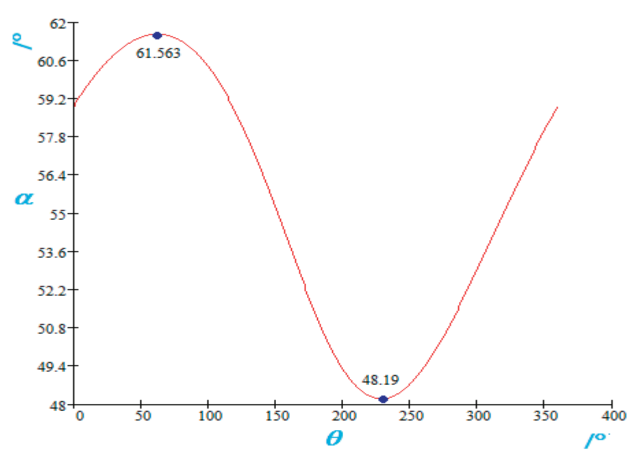

Fig.6 The envelope angle of this test change

3. TEST AND RESULTS

In this test, we designed 4 types of samples, as shown in Fig. 7. There is a fixed contact line between Sample *a* and the eccentric wheel, which simulates the straight-line envelope meshing pair; there are three alternate contact lines between Sample *b* and the eccentric wheel, which simulates the multi-straight line envelope meshing pair; there is a sliding contact line between Sample *c* and the eccentric wheel, which simulates the column (frustum) envelope meshing pair; there is a fixed contact line and a sliding contact line between Sample *d* and the eccentric wheel, which simulates the straight line double envelope meshing pair.

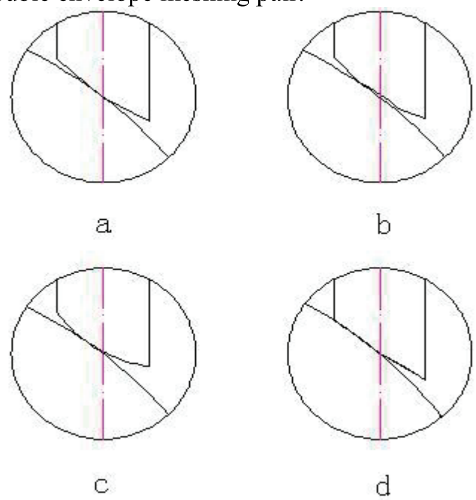

Fig.7 Four types of samples

After wearing, Fig. 8 shows the photo of the samples and Fig. 9 shows the erosion amounts of the different samples. The largest erosion amounts of each sample are shown on Table 2. Comparing the wear resistances in these four samples, sample c has the best anti-wear ability, sample d is better than sample a. So, enlarging the action area of the contact line can enhance wear resistance. Sample b has three alternate contact lines. It should have better performance than sample a. However, in this test, sample b had the largest erosion amount. This is because switching of the three contact lines will cause extra impact load.

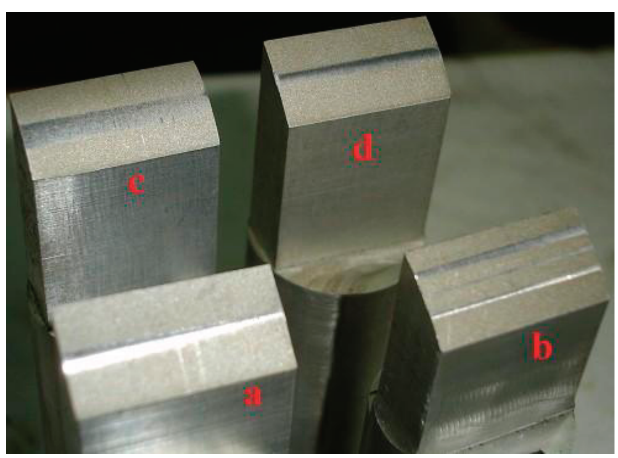

Fig.8 Abrasion of the simples

Table 2: The largest erosion amounts of each different sample

Simple	*a*	*b*	*c*	*d*
The largest erosion amount /mm	0.0048	0.0092	0.0024	0.004

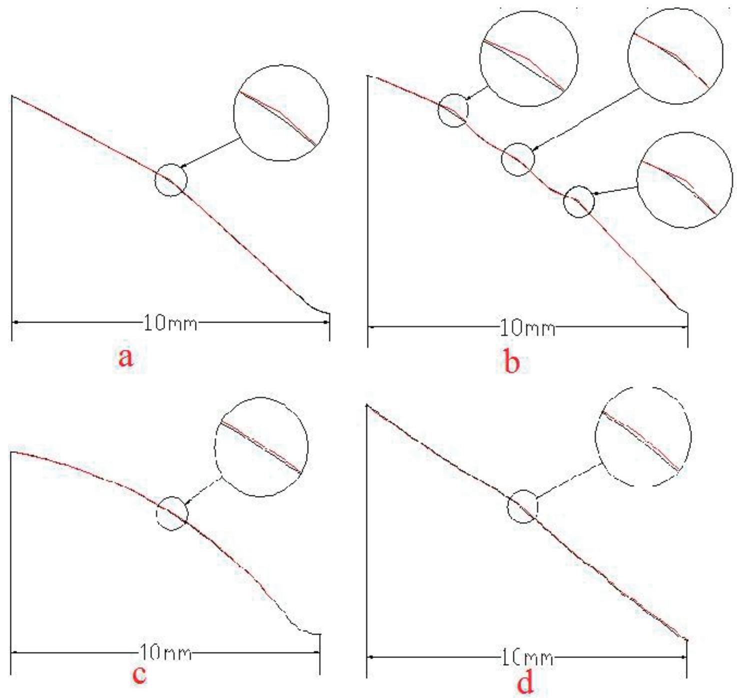

Fig.9 The erosion amounts of the different samples

4. CONCLUSIONS

This work developed a simple eccentric wheel friction test device to compare the wear resistances of different types star-wheel in the SSCs. Choosing appropriate parameters can make the variation range of the envelope angle the same as the envelope angle change range in the SSCs.

The tests indicate that the column (frustum) envelope meshing pair has higher wear resistance than the straight line envelope meshing pair. The impact load, caused by discontinuous loading, will decrease the wear resistance of the multi-straight line envelope meshing pair.

REFERENCES

Wu, Z.Y., Tao, G.L., 2006, Simulation of high speed single screw compressor in fuel cell. *Journal of ZhejiangUniversity (Engineering Science)*, 40(2): 309-312,333 (In Chinese).

Zimmern, B., and Patel, G. C., 1972, Design and Operating Characteristics of the Zimmern Single Screw Compressor, *Compressor Technology Conference*, Purdue, pp. 96–99.

Zimmern, B., 1976, Rotary Injection Worm and Worm Wheel with Specific Tooth Shape. US Patent No. 3932077.

Zimmern, B., 1990, Method and aScrew Machine for Processing Fluid under High Pressure with Liquid Injection Between a Sealing Portion and Support Portion of the Gate Rotor. US Patent No. 4900239.

Zimmern, B., 2000, Single Screw Compressor with Liquid Lock Preventing Slides. US Patent No. 6106241.

Feng, Q.K., Guo, B., *et al*, (2005) A Design Method of Engaging Couple Profile of Single Screw Compressors Enveloped by Multi Straight Line, *Compressor Technology*, 191(03): 1-6 (In Chinese).

Jin, G.X., 1982,, A Study of the Profile and Hydrodynamic Lubrication of a Mono-screw Compressor, *Journal of Xi'an Jiaotong University*, (06):80-82 (In Chinese).

Jin, G.X., Tang Y., 1985, Resent Advances in the Profile Study of the Engagement Pair of a Single-screw Compressor, *Journal of Xi'an Jiaotong University*, 19(6):1-9 (In Chinese).

Wu W.F., Feng Q.K., 2009, A Multicolumn Envelope Meshing Pair for Single Screw Compressors. *Journal of Mechanical Design*, 131 (7).

Kang S.K., Ehmann K.F., Lin C., 1996, A CAD approach to helical groove machining-I Mathematical Model and Model Solution , *International Journal of Machine Tools and Manufacture*, 36 (01): 141-153.